Jefferson.

Thomas Jefferson University
Jefferson Digital Commons

Department of Neuroscience | Sidney Kimmel Medical College

12-11-2013

Defects in synapse structure and function precede motor neuron degeneration in Drosophila models of FUS-related ALS.

Mohammad Shahidullah
Farber Institute for Neurosciences, Thomas Jefferson University, Mohammad.Shahidullah@jefferson.edu

Sylvain J Le Marchand
Vanderbilt University; Thomas Jefferson University, Sylvain.LeMarchand@jefferson.edu

Hong Fei
Department of Neuroscience, Thomas Jefferson University, Hong.Fei@jefferson.edu

Jiaming Zhang

Udai Bhan Pandey
Louisiana State University Health Sciences Center, New Orleans

See next page for additional authors

Let us know how access to this document benefits you

Follow this and additional works at: http://jdc.jefferson.edu/department_neuroscience

 Part of the Neurosciences Commons

Recommended Citation
Shahidullah, Mohammad; Le Marchand, Sylvain J; Fei, Hong; Zhang, Jiaming; Pandey, Udai Bhan; Dalva, Matthew B.; Pasinelli, Piera; and Levitan, Irwin B., "Defects in synapse structure and function precede motor neuron degeneration in Drosophila models of FUS-related ALS." (2013). *Department of Neuroscience.* Paper 10.
http://jdc.jefferson.edu/department_neuroscience/10

This Article is brought to you for free and open access by the Jefferson Digital Commons. The Jefferson Digital Commons is a service of Thomas Jefferson University's Center for Teaching and Learning (CTL). The Commons is a showcase for Jefferson books and journals, peer-reviewed scholarly publications, unique historical collections from the University archives, and teaching tools. The Jefferson Digital Commons allows researchers and interested readers anywhere in the world to learn about and keep up to date with Jefferson scholarship. This article has been accepted for inclusion in Department of Neuroscience by an authorized administrator of the Jefferson Digital Commons. For more information, please contact: JeffersonDigitalCommons@jefferson.edu.

Authors
Mohammad Shahidullah, Sylvain J Le Marchand, Hong Fei, Jiaming Zhang, Udai Bhan Pandey, Matthew B. Dalva, Piera Pasinelli, and Irwin B. Levitan

This article is available at Jefferson Digital Commons: http://jdc.jefferson.edu/department_neuroscience/10

Neurobiology of Disease

Defects in Synapse Structure and Function Precede Motor Neuron Degeneration in *Drosophila* Models of FUS-Related ALS

Mohammad Shahidullah,[1] Sylvain J. Le Marchand,[1] Hong Fei,[1] Jiaming Zhang,[1] Udai Bhan Pandey,[2] Matthew B. Dalva,[1] Piera Pasinelli,[1] and Irwin B. Levitan[1]

[1]Department of Neuroscience and Farber Institute for Neurosciences, Thomas Jefferson University, Philadelphia, Pennsylvania 19107, and [2]Department of Genetics, Louisiana State University Health Sciences Center, New Orleans, Louisiana 70112

Amyotrophic lateral sclerosis (ALS) is an adult-onset neurodegenerative disease that leads invariably to fatal paralysis associated with motor neuron degeneration and muscular atrophy. One gene associated with ALS encodes the DNA/RNA-binding protein Fused in Sarcoma (FUS). There now exist two *Drosophila* models of ALS. In one, human FUS with ALS-causing mutations is expressed in fly motor neurons; in the other, the gene *cabeza* (*caz*), the fly homolog of FUS, is ablated. These FUS-ALS flies exhibit larval locomotor defects indicative of neuromuscular dysfunction and early death. The locus and site of initiation of this neuromuscular dysfunction remain unclear. We show here that in FUS-ALS flies, motor neuron cell bodies fire action potentials that propagate along the axon and voltage-dependent inward and outward currents in the cell bodies are indistinguishable in wild-type and FUS-ALS motor neurons. In marked contrast, the amplitude of synaptic currents evoked in the postsynaptic muscle cell is decreased by >80% in FUS-ALS larvae. Furthermore, the frequency but not unitary amplitude of spontaneous miniature synaptic currents is decreased dramatically in FUS-ALS flies, consistent with a change in quantal content but not quantal size. Although standard confocal microscopic analysis of the larval neuromuscular junction reveals no gross abnormalities, superresolution stimulated emission depletion (STED) microscopy demonstrates that the presynaptic active zone protein bruchpilot is aberrantly organized in FUS-ALS larvae. The results are consistent with the idea that defects in presynaptic terminal structure and function precede, and may contribute to, the later motor neuron degeneration that is characteristic of ALS.

Introduction

Communication between motor neurons and their target muscles is compromised in amyotrophic lateral sclerosis (ALS). Although overt symptoms in humans and mouse models are associated with muscle atrophy after muscle denervation (Ropper and Brown, 2005), the primary defects that precipitate this loss of neuromuscular connectivity remain poorly understood. Most of what we know about the degradation of the neuromuscular synapse in ALS comes from pathological studies in mouse models of superoxide dismutase 1 (SOD1)-mediated ALS. Analysis of disease progression in these mice suggests that ALS starts in the terminal axon, leading to muscle dysfunction and denervation, and proceeds in a retrograde pattern, with degeneration of the proximal motor axon and eventual loss of neuronal cell bodies (Fischer et al., 2004; Dupuis and Loeffler, 2009). This implies that a local defect in the distal portion of the axon and/or the presynaptic terminal is a primary pathogenic event in disease progression. However, little is known about intrinsic changes in mammalian motor neuron excitability and synaptic transmission in ALS, in part because of the challenges of performing electrophysiological recordings *in vivo*.

Mutations in the DNA/RNA-binding protein Fused in Sarcoma (FUS), as well as in other DNA/RNA-binding proteins such as TDP43, have been implicated in both familial and sporadic cases of ALS (Sreedharan et al., 2008; Kwiatkowski et al., 2009; Vance et al., 2009). Recently, models of both FUS-related and TDP43-related ALS have been established both in the fruit fly *Drosophila* (Lanson et al., 2011; Wang et al., 2011; Miguel et al., 2012; Sasayama et al., 2012; Xia et al., 2012) and in zebrafish (Kabashi et al., 2010; Armstrong and Drapeau, 2013a; Armstrong and Drapeau, 2013b). Expression of human disease-causing mutants of either FUS or TDP43 in flies or fish leads to impaired locomotor activity and early death (Kabashi et al., 2010; Lanson et al., 2011). Flies that lack the gene *cabeza* (*caz*), the fly homolog of FUS, exhibit similar phenotypes that can be rescued by the expression of wild-type but not mutant human FUS (Wang et al., 2011), which is consistent with the idea that FUS-mediated ALS involves both loss of nuclear function and gain of toxic function

Received Aug. 8, 2013; revised Oct. 15, 2013; accepted Nov. 1, 2013.

Author contributions: P.P. and I.L. designed research; M.S., S.J.L.M., H.F., J.Z., and M.B.D. performed research; U.P. contributed unpublished reagents/analytic tools; M.S., S.J.L.M., M.B.D., P.P., and I.L. analyzed data; I.L. wrote the paper.

This work was supported by the National Institutes of Health (Grant NS17910 to I.B.L., Grants DA022727 and MH086425 to M.B.D., and Grant NS081303 to U.B.P.) the Robert Packard Center for ALS at Johns Hopkins University (to U.B.P.), the ALS Association (to U.B.P.), and the Farber Family Foundation (to I.B.L. and P.P.).

The authors declare no competing financial interests.

Correspondence should be addressed to Irwin B. Levitan, PhD, Department of Neuroscience, Thomas Jefferson University, 900 Walnut Street, Room 467, Philadelphia, PA 19107. E-mail: Irwin.levitan@jefferson.edu.

DOI:10.1523/JNEUROSCI.3396-13.2013

Copyright © 2013 the authors 0270-6474/13/3319590-09$15.00/0

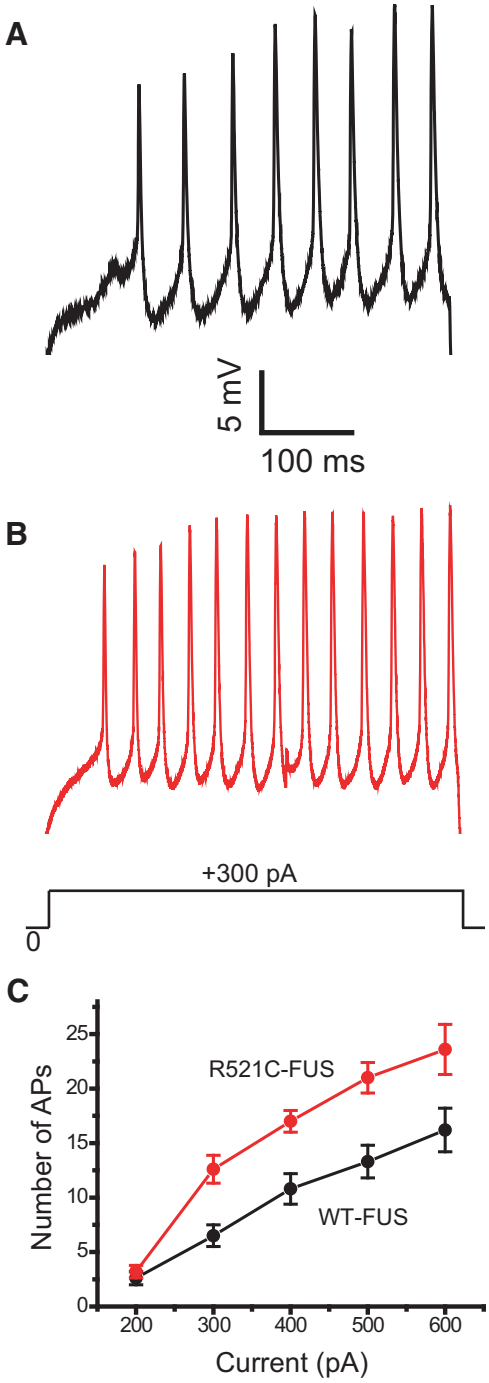

Figure 1. Whole-cell patch recording demonstrates the ability of motor neurons to fire action potentials in response to a depolarizing current injection *in vivo*. Action potentials were evoked in motor neuron cell bodies under current-clamp mode. The starting voltage was adjusted to −80 mV by the injection of an appropriate amount of holding current and action potentials were evoked by the subsequent injection of depolarizing current in neurons expressing either wild-type FUS (***A***) or R521C-FUS (***B***). ***C***, Number of action potentials evoked by different depolarizing current injections in wild-type (black) and R521C-FUS (red) motor neurons. Errors bars indicate SEM. The differences between the two genotypes are significant ($p < 0.05$) at all current injection levels except 200 pA. $n = 6$ for each genotype.

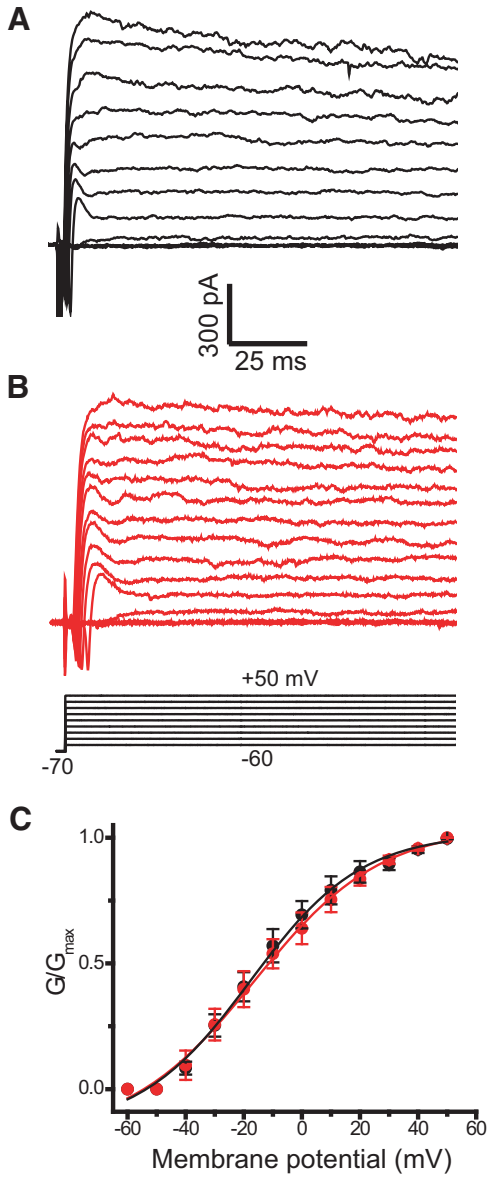

Figure 2. Whole-cell patch recording evokes inward and outward currents in motor neurons *in vivo*. Using voltage-clamp mode, fast inward and large outward currents were evoked by 150 ms depolarizing voltage steps from a holding potential of −70 mV to potentials ranging from −60 to +50 mV in 10 mV increments (***B***, inset), in motor neurons from wild-type (***A***) and R521C-FUS (***B***) flies. All currents were leak subtracted (p/n method) and no differences in leak current between genotypes were observed. ***C***, *G–V* relationships for the peak outward currents in the above genotypes (wild-type, black, $n = 7$; R521C-FUS, red, $n = 5$). Errors bars indicate SEM. There is no significant difference in the *G–V* relationships.

from accumulation of mislocalized cytoplasmic mutant FUS. In the fly, because cell-type-specific drivers are used to restrict the expression of mutant human FUS to motor neurons, it is evident that the locomotor and life span phenotypes must arise from defects in the presynaptic cell. Morphological and electrophysiological analysis of the fish neuromuscular junction also suggests that presynaptic changes accompany the disease phenotype (Armstrong and Drapeau, 2013a).

We have examined motor neuron cell body excitability, axonal conduction, synaptic transmission, and synapse structure in mutant FUS-expressing and *cabeza*-null flies, and report here that neuronal excitability and action potential propagation are essentially normal at the same time that neurotransmitter release is severely impaired and presynaptic active zone structure is aberrant. The results suggest that defects in presynaptic structure and function are early and are perhaps precipitating events in the pathogenesis of FUS-related ALS.

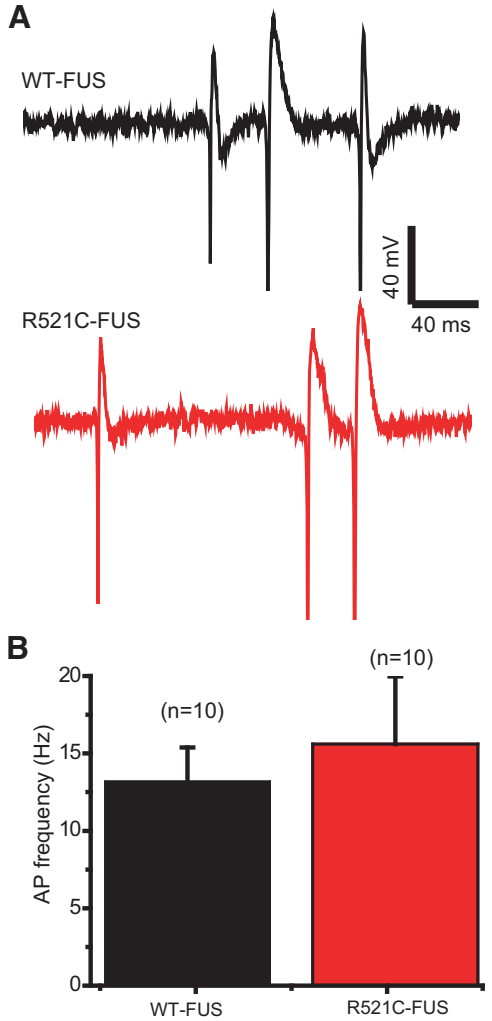

Figure 3. Orthodromic action potentials propagate along the motor neuron axon. ***A***, Spontaneous action potentials recorded under current-clamp mode with a suction electrode on the portion of the severed segmental nerve attached to the ventral ganglion in wild-type FUS- and R521C-FUS-expressing larvae. ***B***, There is no significant difference between genotypes in action potential frequency. $n = 10$ for both genotypes.

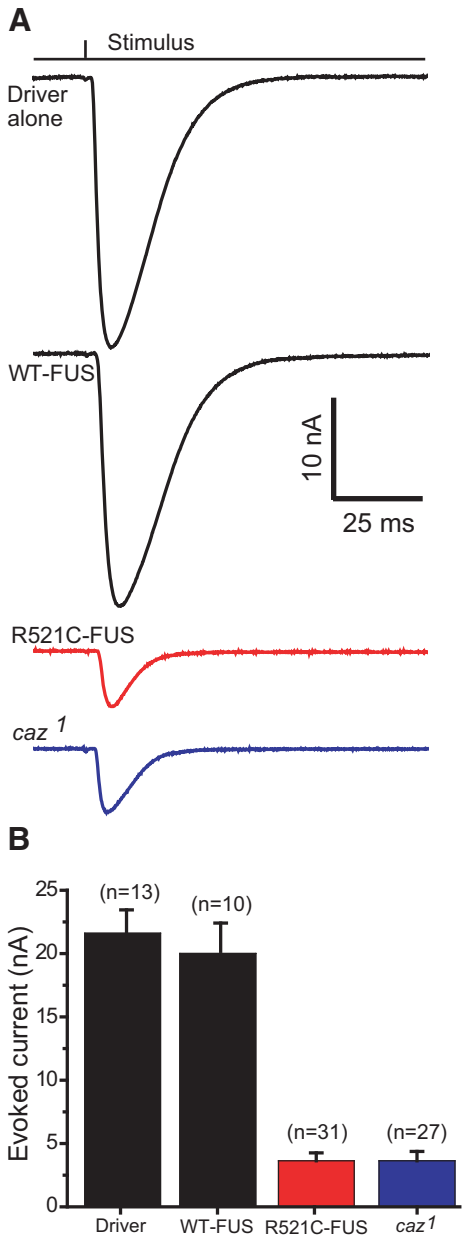

Figure 4. Evoked synaptic transmission at the larval neuromuscular junction. ***A***, Postsynaptic EJCs evoked in the voltage-clamped muscle cell in larvae of the indicated genotypes, by a stimulus (top) applied to the presynaptic segmental nerve. ***B***, Averaged EJC amplitude evoked in larvae of the indicated genotypes. Errors bars indicate SEM. The EJC amplitudes of both R521C-FUS-expressing and *caz*^{1} larvae are significantly less ($p < 0.0001$) than in wild-type FUS or driver-alone larvae.

Materials and Methods

Fly genetics. Flies expressing either wild-type or R521C mutant human FUS as UAS transgenes (Lanson et al., 2011) were crossed with the motor-neuron-specific driver fly line OK371-GAL4 to drive expression of FUS exclusively in motor neurons. *caz*^{1} flies that are null for the gene *caz* (Wang et al., 2011) were generously provided by Dr. Brian McCabe of Columbia University. For some experiments, FUS-expressing flies that express UAS-GFP under the control of the OK371-GAL4 driver were used to identify fluorescent motor neuron cell bodies for electrophysiological recordings. The flies were raised on standard fly food and genetic crosses were performed at 25°C.

Electrophysiological recording from larval motor neuron cell bodies. All experiments were performed on wandering late-third-instar larvae of either sex. Larvae were pinned dorsal side up and bathed in Ca^2-free solution containing the following (in mM): 70 NaCl, 5 KCl, 4 $MgCl_2$, 10 $NaHCO_3$, 5 trehalose, 115 sucrose, and 5 HEPES, pH 7.2. The preparation was visualized using an upright Olympus BX511WI microscope. To access motor neuron cell bodies in the ventral ganglion, Protease 14 (2 mg/ml extracellular solution; Sigma-Aldrich) was focally applied to the ganglionic sheath by applying positive pressure to a recording electrode with the tip broken to a diameter of ~10 μm. Treatment of the sheath was performed with constant laminar perfusion and the debris was removed by applying negative pressure to the electrode. Motor neuron cell bodies were visualized though the expression of a UAS-GFP transgene under the control of the OK371-GAL4 driver. For consistency, we restricted our recordings to the aCC subset of motor neurons identified separately with the RRA-GAL4 driver (Fujioka et al., 2003). The extracellular recording solution contained the following (in mM): 101 NaCl, 3 KCl, 1.8 $CaCl_2$, 2 $MgCl_2$, 1.25 Na_2HPO_4, 5 glucose, and 20.7 $NaHCO_3$, pH 7.2. Thin-walled borosilicate electrodes were pulled to a resistance of 4–6 MΩ when filled with intracellular solution containing the following (in mM): 102 K-gluconate, 17 NaCl, 2 $CaCl_2$, 5 EGTA, 0.5 $MgCl_2$, and 10 HEPES, pH 7.2. Standard techniques were used to record macroscopic currents in the whole-cell voltage-clamp mode and voltage in current-clamp mode with an Axopatch 200A amplifier (Molecular Devices). Data were digitized with a Digidata 1322A interface (Molecular Devices) and

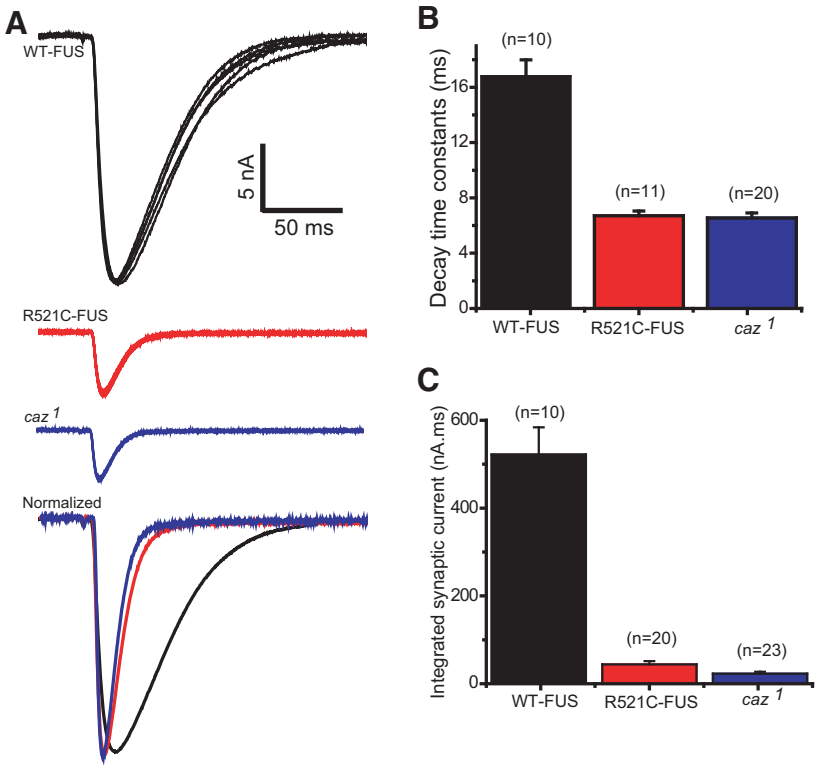

Figure 5. Kinetic analysis of the evoked synaptic currents. ***A***, Five consecutive evoked EJCs from wild-type-FUS (top), R521C-FUS (second), and *caz*^{1} (third) larvae are shown. Bottom: EJCs are averaged, normalized to the peak amplitudes, and superimposed. ***B***, Averaged single exponential time constants fit to the decay phase of the EJC in WT-FUS, R521C-FUS, and *caz*^{1} flies. Both R521C-FUS and *caz*^{1} decay time constants are significantly smaller than in wild-type FUS larvae ($p < 0.0001$). ***C***, Averaged integrated synaptic currents in WT-FUS, R521C-FUS, and *caz*^{1} flies. Integrated synaptic currents were measured by calculating the total area under the EJC. Errors bars indicate SEM. Both R521C-FUS and *caz*^{1} integrated synaptic currents are significantly smaller than in wild-type FUS larvae ($p < 0.0001$).

stored on a PC hard drive for further analysis with pClamp10 software (Molecular Devices).

Synaptic transmission at the larval neuromuscular junction. Larvae were dissected and recorded in hemolymph-like saline HL3.1 containing the following (in mM): 70 NaCl, 5 KCl, 1 $CaCl_2$, 4 $MgCl_2$, 10 $NaHCO_3$, 5 trehalose, 115 sucrose, and 5 HEPES, pH 7.2, as described previously (Broadie and Bate, 1993; Feng et al., 2004; Ueda and Wu, 2006). The segmental nerves were severed from the ventral ganglion and stimulated with a suction electrode. Recordings were performed on ventral longitudinal muscle 6 in abdominal segments A3-A5 of third instar larvae as described previously (Broadie and Bate, 1993). All cells selected for recording had resting membrane potentials between −50 and −70 mV. Both spontaneous and evoked postsynaptic currents were recorded while the muscle cell was voltage clamped at −60 mV using an AxoClamp 2A (Molecular Devices) amplifier in single-electrode voltage-clamp mode (switching frequency 10 kHz) and sharp microelectrodes (catalog #TW150F-3; WPI) filled with 3 M KCl (5–10 MΩ resistance).

Recording of orthodromic action potentials. Larvae were dissected and prepared as above for the measurement of synaptic transmission. The segmental nerve was severed as far from the ventral ganglion as possible and the end attached to the ganglion was drawn into a suction electrode and sealed tightly by the application of negative pressure. Voltage was measured in current-clamp (Track, I = 0) mode with the Axopatch 200A amplifier (Molecular Devices).

Stimulated emission depletion microscopy analysis of the larval neuromuscular junction. Larval neuromuscular preparations were dissected in low-calcium solution of composition containing the following (in mM): 0.2 $CaCl_2$, 70 NaCl, 5 KCl, 20 $MgCl_2$, 10 $NaHCO_3$, 115 sucrose, 5 trehalose, and 5 HEPES, at pH 7.3. Larvae were fixed in 4% paraformaldehyde in PBS for 20 min. Active zones in presynaptic boutons on muscles 6/7 in abdominal segment A3 were visualized using the commercially available monoclonal antibody Nc82, which recognizes Bruchpilot, a *Drosophila* active zone protein homologous to the mammalian active zone component CAST (Kittel et al., 2006). Blocking solution and antibodies were applied in PBS with 0.15% Triton X-100. Stimulated emission depletion (STED) images were obtained with a Leica TCS SP5 STED CW microscope. The Alexa Fluor 488 dye attached to the secondary antibody was excited with a 488 nm laser line and depleted by a 592 nm laser line. STED images were deconvolved using the built-in deconvolution algorithm of the Leica LAS-AF software (i.e., signal intensity filter, regulation parameter: 0.03).

Fractal analysis. Active zones selected for analysis were defined as "doughnut shaped" when a center hole could be visualized by thresholding the image. Images of individual doughnut-shaped active zones were selected for each genotype, converted to binary images, and outlined using ImageJ functions. The complexity of the pattern of each selected active zone contour was determined using ImageJ software with the FracLac plugin (http://imagej.nih.gov/ij/plugins/fraclac/fraclac.html). For each active zone, both the fractal dimension (i.e., by the box-counting method) and the circularity of the convex hull were determined. The fractal dimension provides a measure of shape complexity and, for 2D images, the fractal dimension is usually between 1 and 2. The greater the fractal dimension, the more complex the shape. The convex hull is a boundary enclosing the shape using straight line segments that connect each of its outermost points. The circularity of a shape is between 0 and 1, with 1 being the circularity of a circle. Average active zone shapes, as presented in Figure 9*B*, were obtained by compiling all the active zone binary images to stacks and by projecting the stack images into one image (i.e., "*z* project" function, average intensity).

Results

Electrical excitability of larval motor neuron cell bodies and axons is not impaired in R521C-FUS-expressing flies

To determine the effects of the expression of mutant human FUS on larval motor neuron cell body excitability, we recorded action potential waveforms under current-clamp and voltage-dependent inward and outward currents under voltage clamp. Overshooting action potentials can be evoked in neurons expressing either wild-type (Fig. 1*A*) or R521C mutant human FUS (Fig. 1*B*) by the injection of depolarizing current via the recording electrode (Fig. 1*B*, inset). The neurons of both genotypes fire repetitively in response to a sustained stimulus, with no apparent accommodation. Interestingly, in the R521C-FUS-expressing motor neurons (Fig. 1*B*), more action potentials are evoked by the same depolarizing stimulus at all but the lowest stimulus level examined (Fig. 1*C*). This increase in evoked action potential frequency is not accompanied by a significant change in membrane input resistance or time constant (data not shown). A similar increase in excitability with no change in input resistance has been reported in zebrafish motor neurons that express mutant human TDP43 (Armstrong and Drapeau, 2013a) or FUS (Armstrong and Drapeau,

2013b), as well as in SOD1 mouse models of ALS (Kuo et al., 2004; van Zundert et al., 2008; Fritz et al., 2013).

To examine further the possible influence of mutant FUS on motor neuron membrane excitability, we recorded voltage-dependent currents under voltage clamp. We found that the FUS genotype appears to have little effect on the fast inward currents evoked by membrane depolarization. Furthermore, the large, voltage-dependent outward currents also are very similar in wild-type and R521C-FUS larvae (Fig. 2*A*,*B*) and the conductance–voltage (*G*–*V*) relationships of the peak outward currents are indistinguishable between the two genotypes (Fig. 2*C*). Therefore, the severe impairment in locomotor activity in R521C-FUS-expressing larvae (Lanson et al., 2011; Wang et al., 2011) does not result from an inability of motor neuron cell bodies to generate inward and outward currents or fire action potentials robustly.

To determine whether the action potentials generated in the motor neuron somata can propagate along the axon, we recorded with a suction electrode from the severed end of the segmental nerve that remains attached to the central ganglion. Spontaneous action potentials can be recorded (Fig. 3*A*), which presumably arise in and propagate from the cell bodies. In contrast to the evoked cell body action potentials in Figure 1, there is no statistically significant difference in the frequency of the spontaneous orthodromic action potentials recorded from the axons of wild-type FUS and R521C-FUS-expressing larvae (Fig. 3*B*).

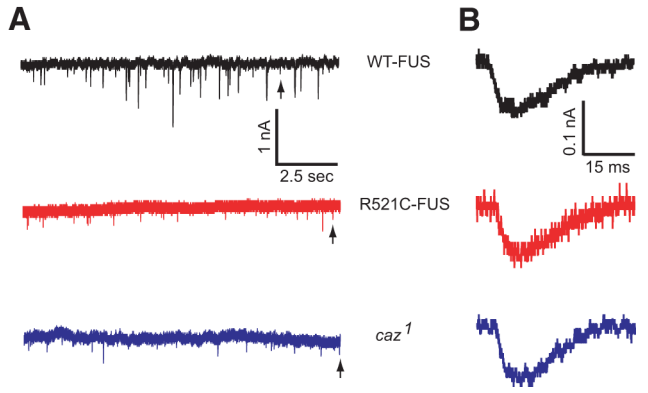

Figure 6. Spontaneous mEJCs in WT-FUS, R521C-FUS, and *caz*^{1} flies. The muscle cell was voltage clamped at −60 mV as for Figure 4, but no stimulus was delivered to the segmental nerve. ***A***, Representative current traces from WT-FUS (top, black), R521C-FUS (middle, red), and *caz*^{1} (bottom, blue) flies. ***B***, Individual mEJCs identified by the arrows in ***A*** are shown at higher time and amplitude resolution. $n = 20$ for each genotype.

Synaptic transmission at the larval neuromuscular junction is severely impaired in R521C-FUS-expressing and *caz*^{1}-null flies

We next examined synaptic transmission at the larval neuromuscular junction by voltage clamping the postsynaptic muscle cell and stimulating the presynaptic segmental nerve. In larvae expressing only the GAL4 driver but no FUS transgene, robust excitatory junctional currents (EJCs) can be evoked by nerve stimulation, and presynaptic expression of wild-type FUS does not influence the amplitude of the EJC (Fig. 4*A*,*B*). In contrast, expression of R521C-FUS in the motor neurons leads to a dramatic decrease in the amplitude of the EJC, and a similar decrease is seen in *caz*^{1}-null flies (Fig. 4*A*,*B*). No such decrease in EJC amplitude is observed in R521C-FUS transgenic larvae in the absence of the GAL4 driver (data not shown), indicating that the synaptic defect is associated with the expression of the mutant protein.

Interestingly, the decay of the EJC is much faster in R521C-expressing and in *caz*^{1} larvae (Fig. 5*A*), with decay time constants that are ~35% of those in the wild-type FUS larvae (Fig. 5*B*). This substantial change in the decay kinetics, in combination with the decrease in EJC amplitude, results in an even more profound decrease in the integrated synaptic current (Fig. 5*C*).

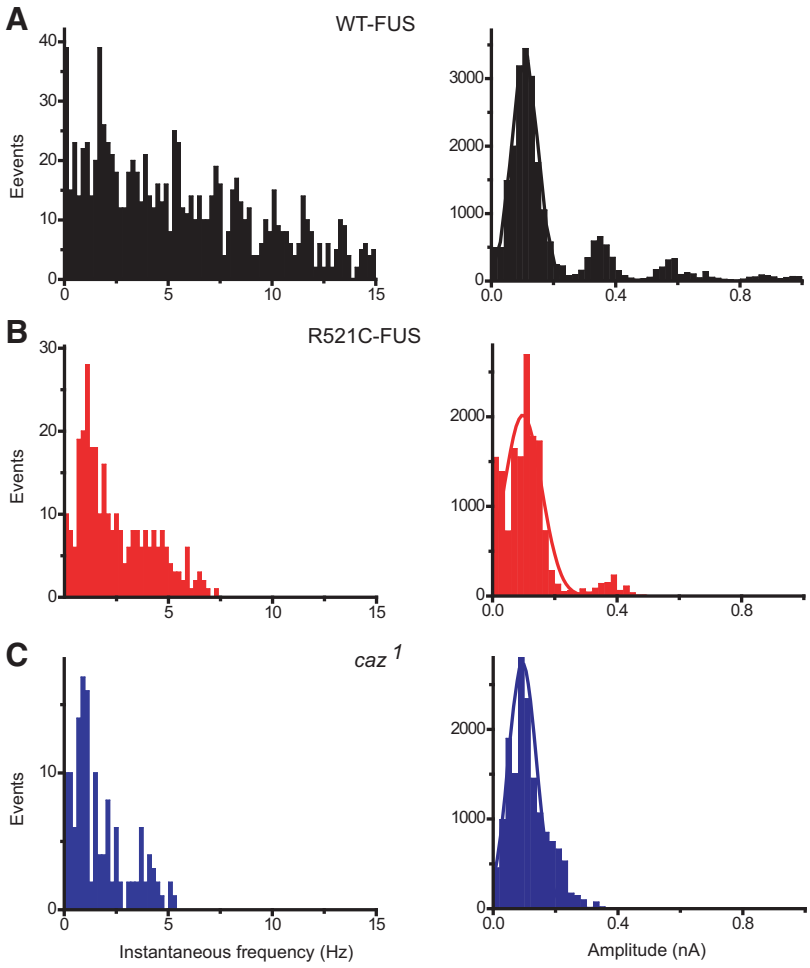

Figure 7. Distributions of mEJC frequencies (left) and amplitudes (right) in WT-FUS (***A***), R521C-FUS (***B***), and *caz*^{1} (***C***) flies. Data are combined from six experiments for each genotype. The instantaneous frequency was calculated as the reciprocal of the interval between individual mEJCs (Benton and Dahanukar, 2011). Bin sizes are 0.2 Hz and 20 pA, respectively. The first 15 bins in each amplitude histogram were fit with a Gaussian function (solid lines).

To further extend the analysis of synaptic transmission, we recorded spontaneous miniature EJCs (mEJCs) from the different fly genotypes. mEJC frequency is used widely as a reliable reporter of presynaptic neurotransmitter release, which often is

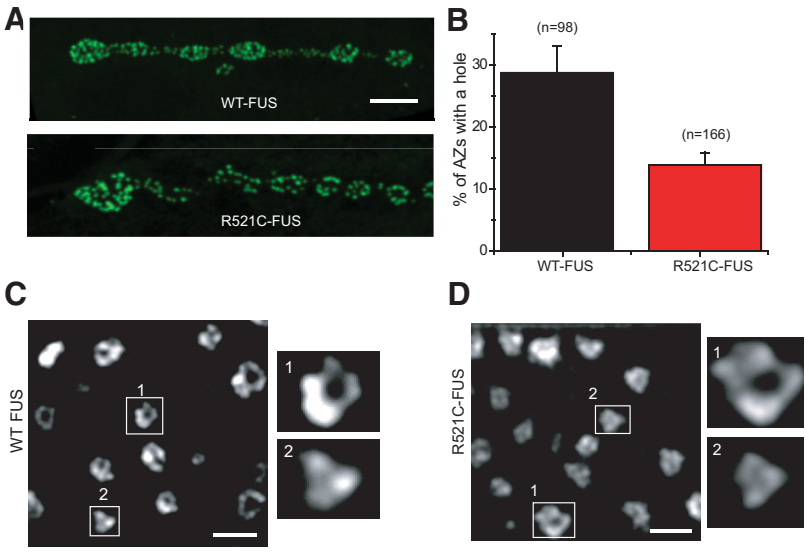

Figure 8. Imaging of presynaptic boutons and active zones at the neuromuscular junction in larvae of the indicated genotypes. ***A***, Confocal imaging of NMJ boutons stained with an antibody that recognizes the active zone marker bruchpilot indicates comparable morphology in wild-type and R521C-FUS-expressing flies. Scale bar, 5 μm. ***B***, Analysis of bruchpilot staining at active zones by STED microscopy reveals that the proportion of active zones (AZs) exhibiting a central hole is reduced in R521C-FUS-expressing flies. Error bars indicate SEM. Statistical significance was evaluated by unpaired Student's *t* test ($p < 0.01$). ***C–D***, Representative STED images of bruchpilot staining at active zones in wild-type and R521C-FUS-expressing flies, respectively. Insets 1, Higher-magnification images of "doughnut-shaped" active zones. Insets 2, Higher-magnification images of active zones without a distinguishable central hole. Scale bars, 0.5 μm.

difficult to measure directly. As shown in the traces in Figure 6*A*, fewer spontaneous mEJCs are observed in R521C-FUS-expressing and *caz*^{1} larvae compared with larvae that express wild-type FUS. However, an examination of individual mEJCs at higher time and amplitude resolution (Fig. 6*B*) suggests that there is no difference among genotypes in the amplitude or kinetics of the unitary mEJC. These conclusions are reinforced by the frequency and amplitude histograms shown in Figure 7. The frequency histograms (Fig. 7, left) demonstrate that the distribution of mEJCs is shifted markedly to the lower-frequency range in both R521C-FUS (Fig. 7*B*) and *caz*^{1} (Fig. 7*C*) flies. Interestingly, although an inspection of the low-time-resolution current traces in Figure 6*A* suggests that mEJC amplitudes are affected by FUS genotype as well, the amplitude histograms (Fig. 7, right) show clearly that the unitary mEJC size is the same in all three genotypes (Fig. 6*B*). Therefore, the apparent difference in mEJC amplitudes (Fig. 6*A*) reflects the higher frequency of mEJCs and simultaneous release of several synaptic vesicles in the wild-type larvae (note the higher amplitude peaks in Fig. 7*A*, right). The Gaussian fits to the first peak in each amplitude histogram yield amplitude values of 100 ± 41 pA (mean ± width at half-peak amplitude) in wild-type FUS larvae, 97 ± 59 pA in R521C-FUS larvae, and 93 ± 45 pA in *caz*^{1} larvae. Therefore, quantal size is unchanged by R521C-FUS expression or *caz* ablation, but the number of synaptic vesicles undergoing evoked release (quantal content, defined as evoked EJC amplitude/unitary mEJC amplitude) decreases from 200 in WT-FUS flies to 37 and 39 in R521C-FUS and *caz*^{1} flies, respectively.

Structure of presynaptic active zones is aberrant in R521C-FUS-expressing flies

As yet, there is no consensus as to whether fly models of FUS- or TDP43-related ALS exhibit morphological defects at the larval neuromuscular junction, as measured by confocal microscopy. As shown previously (Lanson et al., 2011), expression of mutant human FUS does not affect presynaptic bouton number or overall synaptic morphology, and *caz*^{1}-null flies were reported to have normal neuromuscular junction morphology as well (Wang et al., 2011). However, aberrant synaptic morphology has been described in flies lacking *caz* or expressing both wild-type and mutant human FUS (Xia et al., 2012). In the present study, confocal imaging revealed no obvious differences in bouton size or number between wild-type FUS and R521-FUS-expressing flies (Fig. 8*A*), but we did not investigate this in depth. Instead, we imaged the presynaptic active zone protein bruchpilot using superresolution STED microscopy. Consistent with previous work in wild-type flies (Kittel et al., 2006), STED imaging of bruchpilot in wild-type FUS transgenic flies reveals that it is localized in structures thought to be individual active zones, many of which are doughnut shaped (Fig. 8*C*). Presynaptic calcium channels critical for neurotransmitter release are thought to be localized within the central doughnut holes (Liu et al., 2011). Transgenic flies expressing R521C-FUS appear to have normal numbers of bruchpilot-positive active zones, but the pattern of bruchpilot staining is different (Fig. 8*D*). First, there is a 50% reduction in the number of active zones with discernible doughnut holes in R521C-FUS flies (Fig. 8*B*). In addition, the bruchpilot-labeled structures appear disorganized, as they are in flies lacking RIM-binding protein, a key protein component of active zones (Liu et al., 2011).

To determine quantitatively whether bruchpilot-labeled active zones with discernible doughnut holes are misshapen in R521C-FUS flies compared with those in wild-type FUS transgenic flies, we examined the relationship between the size of the central hole and overall active zone area and used a fractal-based analysis to generate a quantitative measure of the complexity of the active zones. Examples of individual active zones in the two genotypes are outlined in Figure 9*A* and averaged active zones are shown in Figure 9*B*. The areas of individual active zones are similar in wild-type FUS and R521C-FUS-expressing flies (Fig. 9*C*). However, the overall size of the bruchpilot active zone is less well correlated with the size of the doughnut hole in the R521C-FUS flies (Fig. 9*D*). Furthermore, fractal analysis of the active zones indicates that they are significantly less complex (Fig. 9*E*) and more circular (Fig. 9*F*) in R521C-FUS than in wild-type FUS transgenic flies. In sum, superresolution microscopy reveals that active zones in R521C-FUS flies are aberrantly organized and misshapen compared with their wild-type counterparts.

Discussion

The demonstration that mutations in the DNA/RNA-binding proteins TDP43 and FUS are associated with both familial and sporadic ALS has profoundly influenced thinking about the pathogenesis of the disease (for reviews, see Lagier-Tourenne and Cleveland, 2009; Polymenidou et al., 2012). It is becoming evident that the impact of these findings will not be restricted to ALS, because mutations in these same proteins are implicated in at least one other neurodegenerative disorder, frontotemporal

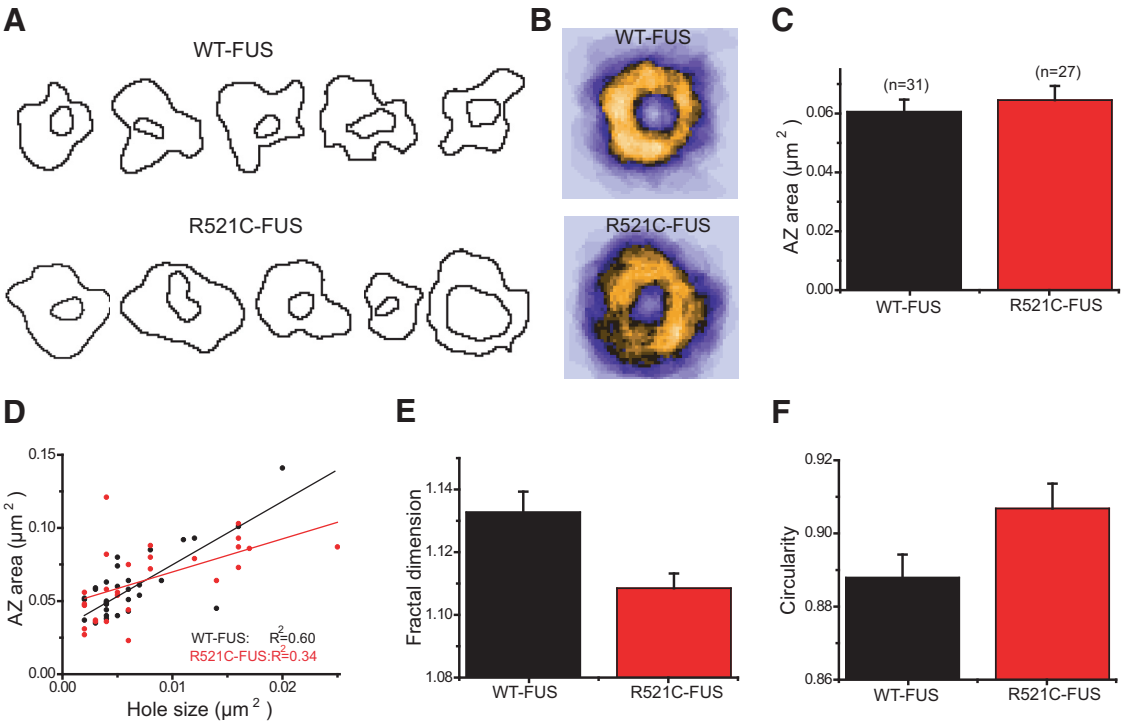

Figure 9. Shape analysis of active zones in wild-type and R521C-FUS-expressing flies. ***A***, Examples of outlines from "doughnut-shaped" bruchpilot stained active zones used for fractal analysis. The first outlines shown on the left for wild-type FUS and R521C-FUS were obtained from the STED images presented in Figure 8*C*, Inset 1, and Figure 8*D*, Inset 1, respectively. ***B***, Averaged shapes obtained from 31 wild-type FUS active zones (top) and 27 R521C-FUS active zones (bottom). ***C***, The average area of "doughnut-shaped" active zones (AZ area) is not different in wild-type FUS and R521C-FUS-expressing flies. ***D***, AZ area and hole size are better correlated in wild-type FUS compared with R521C-FUS active zones, as indicated by the R^2 of the linear regression plots. ***E***, Measurements of the fractal dimension (i.e., box-counting dimension) of AZ shapes reveals that wild-type FUS active zones exhibit a higher degree of complexity compared with R521C-FUS active zones. Errors bars indicate SEM. Statistical significance was evaluated by unpaired Student's *t* test ($p < 0.01$). ***F***, Fractal analysis of AZ shapes indicates that R521C-FUS active zones are more circular than wild-type FUS active zones, as assessed by the circularity of the convex hull ($p < 0.05$).

lobar degeneration (Arai et al., 2006; Neumann et al., 2004). Despite the enormous interest generated by these findings, the mechanisms by which TDP43 and FUS lead to disease onset and progression remain poorly understood. Both are multifunctional proteins that participate in transcriptional regulation and in several aspects of mRNA processing, splicing, transport, and perhaps local translation at the synapse and they may bind to and influence noncoding RNAs as well (Polymenidou et al., 2012).

Several animal models of FUS/TDP43-related ALS are becoming very useful for investigating cellular and molecular aspects of disease progression (Lanson and Pandey, 2012). Transgenic rats that express R521C but not wild-type human FUS exhibit a progressive paralysis and degeneration of motor neurons, as well as neuronal loss in the cortex and hippocampus (Huang et al., 2011). In the zebrafish, a more genetically tractable vertebrate model, expression of mutant human TDP43 or FUS causes disruption of motor neuron projections, larval motor deficits, and synaptic dysfunction (Kabashi et al., 2010; Armstrong and Drapeau, 2013a; Armstrong and Drapeau, 2013b). Finally, several groups have exploited the power of *Drosophila* genetics to produce flies that express either wild-type or mutant human FUS transgenes and have found that expression of the mutant protein leads to locomotor impairment and neurodegeneration (Lanson et al., 2011; Xia et al., 2012). The fly model confers the enormous advantage of being able to restrict expression of the mutant FUS exclusively to the presynaptic motor neuron. Interestingly, expression of the wild-type protein also produces some disease-like phenotypes, but they appear to be later in onset and less severe. Knock-out of *caz*, the gene that encodes the fly homolog of FUS, produces behavioral and morphological defects similar to those caused by transgenic expression of mutant human FUS (Wang et al., 2011; Xia et al., 2012).

We show here that the motor neuron cell bodies of R521C-FUS-expressing larvae generate normal voltage-dependent inward and outward currents and fire action potentials in response to depolarizing stimuli. Furthermore, these action potentials can propagate normally along the axon. Indeed, if anything, the FUS-ALS motor neurons are somewhat more excitable than neurons that express wild-type FUS, again in agreement with the results in zebrafish (Armstrong and Drapeau, 2013a; Armstrong and Drapeau, 2013b) and prior findings in SOD1 mice (Kuo et al., 2004; van Zundert et al., 2008; Fritz et al., 2013). The biophysical mechanism of this widely observed increase in motor neuron excitability in ALS models remains to be determined.

Despite the fact that motor neuron cell body and axon excitability are normal or enhanced, we find that synaptic function at the larval neuromuscular junction is profoundly impaired in flies that overexpress R521C-FUS, as well as in *caz*-null flies. Evoked synaptic transmission is decreased by >80% and spontaneous mEJC frequency is also reduced substantially. These findings reinforce those reported for the zebrafish larval neuromuscular junction after expression of mutant human TDP43 (Armstrong and Drapeau, 2013a) or FUS (Armstrong and Drapeau, 2013b). In the fly, although we cannot be certain whether the effect of *caz* knock-out is pre- or postsynaptic, the changes we observe in mEJC frequency strongly suggest a major presynaptic contribution; a similar inference has been drawn in the zebrafish. Furthermore, in the fly, there is no uncertainty about the primary

presynaptic locus in the case of R521C-FUS expression because the OK-371GAL4 driver restricts expression to the presynaptic motor neuron and, again, mEJC frequency is decreased substantially. Quantal analysis reveals that the unitary mEJC amplitude is the same in R521C-FUS-expressing and *caz*^{1} larvae as in larvae expressing wild-type FUS. This lack of change in quantal size suggests that the size and neurotransmitter content of synaptic vesicles is not affected by FUS genotype. Rather, the decrease in evoked synaptic transmission in the FUS-ALS larvae is most readily explained by a decrease in quantal content, the number of vesicles released in response to a given stimulus. Such a decrease in evoked release probability is consistent with the decrease in spontaneous mEJC frequency observed in the FUS-ALS larvae.

It is surprising and intriguing that the decay of the evoked EJC is considerably faster in the R521C-FUS and *caz*^{1} larvae. Such a change in the kinetics of the EJC might be consistent with a change in the deactivation properties of the postsynaptic glutamate receptors, perhaps secondary to the initial presynaptic defect. Conversely, another possibility is that presynaptic glutamate uptake systems are among the many targets of FUS and are altered in R521C-FUS-expressing and *caz*^{1} motor neurons and that this accounts for the changes in EJC kinetics. A detailed analysis of glutamate receptor properties and glutamate diffusion and reuptake will be required to distinguish between these interesting possibilities and to explain how the kinetics of the evoked EJC are altered by FUS genotype whereas those of the unitary mEJC are not.

Examination of presynaptic bouton structure by confocal microscopy did not reveal any gross morphological abnormalities in the present study or in Lanson et al. (2011) (but see Xia et al., 2012). In contrast, using STED microscopy, we show that the presynaptic active zones, measured by staining the active zone protein bruchpilot, are misshapen and disorganized in R521C-FUS larvae. Although bruchpilot itself is essential for the formation of active zones and neurotransmitter release (Kittel et al., 2006), we use it here as a marker of active zone organization, as has been done previously (Liu et al., 2011). Misshapen bruchpilot-labeled active zones like those we observe in R521C-FUS-expressing larvae are associated with impaired calcium channel clustering and a decrease in calcium influx (Liu et al., 2011) and, in the zebrafish, treatment with calcium channel agonists can rescue both locomotor and synaptic transmission defects induced by expression of mutant TDP43 (Armstrong and Drapeau, 2013a). It will be interesting to use STED microscopy to examine calcium channel organization at active zones in FUS-aberrant *Drosophila* larvae.

Our results demonstrate clearly that structural abnormalities at the synapse and defects in neurotransmitter release precede motor neuron cell body and axonal degeneration in two fly models of FUS-related ALS. Many questions remain to be explored, including the identity of the critical FUS target(s), the mechanism by which overexpression of mutant FUS and knock-out of endogenous *caz* both produce the same synaptic phenotype, and the way that synaptic dysfunction leads ultimately to motor neuron degeneration. Our findings and those in the zebrafish point to the importance of early therapeutic intervention at the synapse in developing novel treatments for ALS.

References

Arai T, Hasegawa M, Akiyama H, Ikeda K, Nonaka T, Mori H, Mann D, Tsuchiya K, Yoshida M, Hashizume Y, Oda T (2006) TDP-43 is a component of ubiquitin-positive tau-negative inclusions in frontotemporal lobar degeneration and amyotrophic lateral sclerosis. Biochem Biophys Res Commun 351:602–611. CrossRef Medline

Armstrong GA, Drapeau P (2013a) Calcium channel agonists protect against neuromuscular dysfunction in a genetic model of TDP-43 mutation in ALS. J Neurosci 33:1741–1752. CrossRef Medline

Armstrong GA, Drapeau P (2013b) Loss and gain of FUS function impair neuromuscular synaptic transmission in a genetic model of ALS. Hum Mol Genet 22:4282–4292. CrossRef Medline

Benton R, Dahanukar A (2011) Electrophysiological recording from *Drosophila* taste sensilla. Cold Spring Harb Protoc 2011:839–850. CrossRef Medline

Broadie KS, Bate M (1993) Development of the embryonic neuromuscular synapse of *Drosophila* melanogaster. J Neurosci 13:144–166. Medline

Dupuis L, Loeffler JP (2009) Neuromuscular junction destruction during amyotrophic lateral sclerosis: insights from transgenic models. Curr Opin Pharmacol 9:341–346. CrossRef Medline

Feng Y, Ueda A, Wu CF (2004) A modified minimal hemolymph-like solution, HL3.1, for physiological recordings at the neuromuscular junctions of normal and mutant *Drosophila* larvae. J Neurogenet 18:377–402. CrossRef Medline

Fischer LR, Culver DG, Tennant P, Davis AA, Wang M, Castellano-Sanchez A, Khan J, Polak MA, Glass JD (2004) Amyotrophic lateral sclerosis is a distal axonopathy: evidence in mice and man. Exp Neurol 185:232–240. CrossRef Medline

Fritz E, Izaurieta P, Weiss A, Mir FR, Rojas P, Gonzalez D, Rojas F, Brown RH Jr, Madrid R, van Zundert B (2013) Mutant SOD1-expressing astrocytes release toxic factors that trigger motoneuron death by inducing hyperexcitability. J Neurophysiol 109:2803–2814. CrossRef Medline

Fujioka M, Lear BC, Landgraf M, Yusibova GL, Zhou J, Riley KM, Patel NH, Jaynes JB (2003) Even-skipped, acting as a repressor, regulates axonal projections in *Drosophila*. Development 130:5385–5400. CrossRef Medline

Huang C, Zhou H, Tong J, Chen H, Liu YJ, Wang D, Wei X, Xia XG (2011) FUS transgenic rats develop the phenotypes of amyotrophic lateral sclerosis and frontotemporal lobar degeneration. PLoS Genet 7:e1002011. CrossRef Medline

Kabashi E, Lin L, Tradewell ML, Dion PA, Bercier V, Bourgouin P, Rochefort D, Bel Hadj S, Durham HD, Vande Velde C, Rouleau GA, Drapeau P (2010) Gain and loss of function of ALS-related mutations of TARDBP (TDP-43) cause motor deficits in vivo. Hum Mol Genet 19:671–683. CrossRef Medline

Kittel RJ, Wichmann C, Rasse TM, Fouquet W, Schmidt M, Schmid A, Wagh DA, Pawlu C, Kellner RR, Willig KI, Hell SW, Buchner E, Heckmann M, Sigrist SJ (2006) Bruchpilot promotes active zone assembly, Ca^{2+} channel clustering, and vesicle release. Science 312:1051–1054. CrossRef Medline

Kuo JJ, Schonewille M, Siddique T, Schults AN, Fu R, Bär PR, Anelli R, Heckman CJ, Kroese AB (2004) Hyperexcitability of cultured spinal motoneurons from presymptomatic ALS mice. J Neurophysiol 91:571–575. CrossRef Medline

Kwiatkowski TJ Jr, Bosco DA, Leclerc AL, Tamrazian E, Vanderburg CR, Russ C, Davis A, Gilchrist J, Kasarskis EJ, Munsat T, Valdmanis P, Rouleau GA, Hosler BA, Cortelli P, de Jong PJ, Yoshinaga Y, Haines JL, Pericak-Vance MA, Yan J, Ticozzi N, Siddique T, McKenna-Yasek D, Sapp PC, Horvitz HR, Landers JE, Brown RH Jr (2009) Mutations in the FUS/TLS gene on chromosome 16 cause familial amyotrophic lateral sclerosis. Science 323:1205–1208. CrossRef Medline

Lagier-Tourenne C, Cleveland DW. Rethinking ALS: the FUS about TDP-43 (2009) Cell 136:1001–1004.

Lanson NA Jr, Pandey UB (2012) FUS-related proteinopathies: lessons from animal models. Brain Res 1462:44–60. CrossRef Medline

Lanson NA Jr, Maltare A, King H, Smith R, Kim JH, Taylor JP, Lloyd TE, Pandey UB (2011) A *Drosophila* model of FUS-related neurodegeneration reveals genetic interaction between FUS and TDP-43. Hum Mol Genet 20:2510–2523. CrossRef Medline

Liu KS, Siebert M, Mertel S, Knoche E, Wegener S, Wichmann C, Matkovic T, Muhammad K, Depner H, Mettke C, Bückers J, Hell SW, Müller M, Davis GW, Schmitz D, Sigrist SJ (2011) RIM-binding protein, a central part of the active zone, is essential for neurotransmitter release. Science 334:1565–1569. CrossRef Medline

Miguel L, Avequin T, Delarue M, Feuillette S, Frébourg T, Campion D, Lecourtois M (2012) Accumulation of insoluble forms of FUS protein correlates with toxicity in *Drosophila*. Neurobiol Aging 33:1008.e1–15. CrossRef Medline

Neumann M, Müller V, Kretzschmar HA, Haass C, Kahle PJ (2004) Re-

gional distribution of proteinase K-resistant alpha-synuclein correlates with Lewy body disease stage. J Neuropathol Exp Neurol 63:1225–1235. Medline

Polymenidou M, Lagier-Tourenne C, Hutt KR, Bennett CF, Cleveland DW, Yeo GW (2012) Misregulated RNA processing in amyotrophic lateral sclerosis. Brain Res 1462:3–15. CrossRef Medline

Ropper AH, Brown RJ (2005) Adams and Victor's principles of neurology. New York: McGraw-Hill.

Sasayama H, Shimamura M, Tokuda T, Azuma Y, Yoshida T, Mizuno T, Nakagawa M, Fujikake N, Nagai Y, Yamaguchi M (2012) Knockdown of the *Drosophila* Fused in sarcoma (FUS) homologue causes deficient locomotive behavior and shortening of motoneuron terminal branches. PLoS One 7:e39483. CrossRef Medline

Sreedharan J, Blair IP, Tripathi VB, Hu X, Vance C, Rogelj B, Ackerley S, Durnall JC, Williams KL, Buratti E, Baralle F, de Belleroche J, Mitchell JD, Leigh PN, Al-Chalabi A, Miller CC, Nicholson G, Shaw CE (2008) TDP-43 mutations in familial and sporadic amyotrophic lateral sclerosis. Science 319:1668–1672. CrossRef Medline

Ueda A, Wu CF (2006) Distinct frequency-dependent regulation of nerve terminal excitability and synaptic transmission by IA and IK potassium channels revealed by *Drosophila* Shaker and Shab mutations. J Neurosci 26:6238–6248. CrossRef Medline

van Zundert B, Peuscher MH, Hynynen M, Chen A, Neve RL, Brown RH Jr, Constantine-Paton M, Bellingham MC (2008) Neonatal neuronal circuitry shows hyperexcitable disturbance in a mouse model of the adult-onset neurodegenerative disease amyotrophic lateral sclerosis. J Neurosci 28:10864–10874. CrossRef Medline

Vance C, Rogelj B, Hortobágyi T, De Vos KJ, Nishimura AL, Sreedharan J, Hu X, Smith B, Ruddy D, Wright P, Ganesalingam J, Williams KL, Tripathi V, Al-Saraj S, Al-Chalabi A, Leigh PN, Blair IP, Nicholson G, de Belleroche J, Gallo JM, Miller CC, Shaw CE (2009) Mutations in FUS, an RNA processing protein, cause familial amyotrophic lateral sclerosis type 6. Science 323:1208–1211. CrossRef Medline

Wang JW, Brent JR, Tomlinson A, Shneider NA, McCabe BD (2011) The ALS-associated proteins FUS and TDP-43 function together to affect *Drosophila* locomotion and life span. J Clin Invest 121:4118–4126. CrossRef Medline

Xia R, Liu Y, Yang L, Gal J, Zhu H, Jia J (2012) Motor neuron apoptosis and neuromuscular junction perturbation are prominent features in a *Drosophila* model of Fus-mediated ALS. Mol Neurodegener 7:10. CrossRef Medline